

## Evolution of microstructure in semi-solid slurries of rheocast aluminum alloy

R. CANYOOK<sup>1</sup>, S. PETSUT<sup>1</sup>, S. WISUTMETHANGOON<sup>2</sup>, M. C. FLEMINGS<sup>3</sup>, J. WANNASIN<sup>1</sup>

1. Department of Mining and Materials Engineering, Faculty of Engineering,  
Prince of Songkla University, Hat Yai, Songkhla, 90112, Thailand;

2. Department of Mechanical Engineering, Faculty of Engineering,  
Prince of Songkla University, Hat Yai, Songkhla, 90112, Thailand;

3. Department of Materials Science and Engineering, Massachusetts Institute of Technology,  
Cambridge, MA 02139, USA

Received 13 May 2010; accepted 25 June 2010

**Abstract:** Semi-solid metal processing is being developed in die casting applications to give several cost benefits. To efficiently apply this emerging technology, it is important to understand the evolution of microstructure in semi-solid slurries for the control of the rheological behavior in semi-solid state. An experimental apparatus was developed which can capture the grain structure at different times at early stages to understand how the semi-solid structure evolves. In this technique, semi-solid slurry was produced by injecting fine gas bubbles into the melt through a graphite diffuser during solidification. Then, a copper quenching mold was used to draw some semi-solid slurry into a thin channel. The semi-solid slurry was then rapidly frozen in the channel giving the microstructure of the slurry at the desired time. Samples of semi-solid 356 aluminum alloy were taken at different gas injection times of 1, 5, 10, 15, 20, 30, 35, 40, and 45 s. Analysis of the microstructure suggests that the fragmentation by remelting mechanism should be responsible for the formation of globular structure in this rheocasting process.

**Key words:** microstructure evolution; rheocasting; rapid quenching method; 356 aluminum alloy; gas induced semi-solid (GISS); formation mechanism

### 1 Introduction

Semi-solid metal (SSM) processing has been used for about 40 years in the metal casting industry to produce higher quality parts than conventional die casting with lower cost than forging processes. Two SSM processing routes are used industrially: thixocasting and rheocasting. Thixocasting can yield high-quality parts with high mechanical properties. However, the costs of the aluminum feedstock billets, reheating system, and forming machines are quite high. However, the recent trend in semi-solid metal processing is focused on applying the rheocasting route[1]. This is because rheocasting can offer cost advantages over thixocasting. In this SSM route, liquid alloy is processed into semi-solid metal at the production site and scrap metals can be recycled in-house[1].

To efficiently apply the rheocasting process, it is important that the quality of the slurry is carefully controlled during the production. In addition, it is

desirable that the process is efficient in producing semi-solid metal in a short time with homogeneous and globular microstructure[2]. To achieve these requirements, it is important to understand the mechanism of the formation of globular structure during rheocasting processes.

In literatures, it is well accepted that the globular microstructure is obtained when a large number of solid grains are formed during the early stages of solidification[3]. The high density of the solid grains results in non-dendritic growth and, therefore, globular microstructure is achieved. However, it is still unclear how these numerous solid grains are formed[4].

Two theories are often proposed by many researchers: copious nucleation and fragmentation. Some researchers[5–9] proposed that the globular grains form directly through direct nucleation and growth. Others[10–14] proposed that the grains come from fragmented dendrite arms. These previous studies in the literatures[5–14] confirm that there are still disagreements among the researchers regarding the

mechanism responsible for forming the numerous solid grains in the semi-solid microstructure. In order to understand the formation mechanism, it is important to study the microstructure evolution at the early stages.

This work aims to investigate the microstructure evolution during the early stages of solidification using a rapid quenching mold technique previously used by several investigators[1].

## 2 Theory

Two mechanisms that are often proposed to explain the formation of a high density of solid particles are copious nucleation and fragmentation.

### 2.1 Copious nucleation mechanism

This mechanism proposes that the numerous grains are obtained as a result of copious nucleation that is achieved by rapid and continuous heat extraction and melt convection. Crucible walls, cold immersed solid surfaces, or inoculant surfaces provide effective heterogeneous nucleation sites for the solid grains to form. Grain nucleation requires a minimum amount of undercooling to be effective so most potential nucleation sites become inactive when the local temperature rises due to the release of latent heat from the previously nucleated grains nearby. As a consequence, only a small fraction of nuclei are formed[4]. Rapid and continuous heat extraction near these surfaces helps to remove the released latent heat, consequently, allowing more nuclei to form. Some of the literatures supporting this mechanism are as follows.

Researchers at C.I.T.[6] investigated a new semi-solid casting process for Cu-Sn alloys using an inclined cooling plate. They proposed the crystal separation theory, explaining that the granular crystals nucleate and grow on the chill mold wall and separate from it due to the fluid motion. The theory is shown schematically in Fig.1. LI et al[7] investigated the morphological evolution during solidification under stirring of succinonitrile-5% water (molar fraction) by in situ observation. They reported that the globular crystals form through direct nucleation and growth from the stirred melt when the alloy is cooled and stirred from a temperature above the liquidus or between the liquidus and solidus. WU et al[8] created semi-solid metal of an Al-Si alloy by introducing mechanical vibration during isothermal holding for 5 min. They suggested that numerous nuclei formed in the melt because of undercooling. Also, many nuclei formed on the crucible wall and then were transported into the bulk melt. JIAN et al[9] evaluated the effect of ultrasonic vibration on the nucleation and growth of aluminum alloy A356 melt. They concluded that the dominant mechanism for the

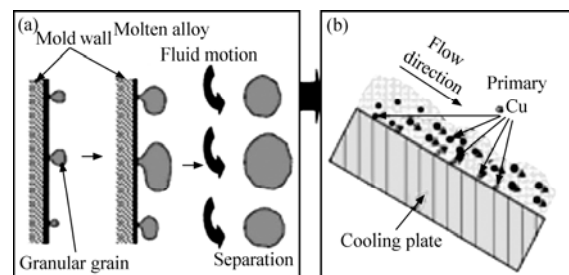


**Fig.1** Schematic of crystal separation theory (a) and principle of generation of new semi-solid slurry using inclined cooling plate (b)[6]

formation of a globular microstructure was likely not due to the fragmentation mechanism, but heterogeneous nucleation induced by cavitation.

### 2.2 Fragmentation mechanism

This mechanism proposes that the high density of solid grains is created from detached secondary or tertiary arms due to solute enrichment and thermo-solutal convection near the dendrite root. FLEMINGS et al[10] suggested that vigorous stirring and localized rapid cooling can provide significant temperature disturbances in a molten metal, which is helpful for the remelting and separation of dendrite arms from a “mother” dendrite. This action as illustrated schematically in Fig.2 leads to grain multiplication. Some of the researches that support this mechanism are as follows.

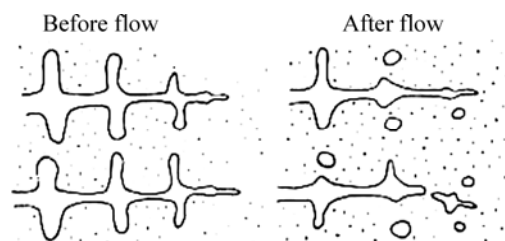


**Fig.2** Schematic diagram of dendrite multiplication[10]

HELLAWELL et al[11] presented a detailed discussion on dendrite fragmentation and the effects of fluid flow in casting. They proposed that remelting of dendrite arms at their roots, rather than breaking off by a mechanical force, might be the cause of grain multiplication. JACKSON et al[12] found that the high solute concentration in the boundary adjacent to the primary phase will lower the local melting temperature. If the solute concentration is changed by the flow, the local melting temperature will be lowered and remelting may occur. JI[13] investigated the dendrite fragmentation in Sn-15%Pb (mass fraction) alloy under shearing using a twin-screw extruder. He suggested that the dendrites are fragmented via the penetration of liquid into the bent

dendrite arms to form large angle grooves along grain boundaries. Later, RUVALCABA et al[14] applied high-brilliance synchrotron X-radiation microscopy and image processing for in situ observations of local solute-enrichment during fragmentation of dendrite arms. The study was done under normal non-forced convection conditions during directional solidification of an Al-20% Cu (mass fraction) alloy. They found that local fragmentation is initiated by transient growth conditions. This occurs naturally during solidification, in which the solute is transported into the mush by gravity-induced liquid flow.

### 3 Experimental

The commercial 356 aluminium alloy was used in this study. The chemical composition of this alloy is given in Table 1. The liquidus temperature of the alloy is 613 °C, and the eutectic temperature is 573 °C.

**Table 1** Chemical composition of 356 aluminium alloy in this study (mass fraction, %)

| Si   | Fe   | Cu   | Mn   | Mg   | Zn   | Ti   | Ni   | Al   |
|------|------|------|------|------|------|------|------|------|
| 6.90 | 0.41 | 0.05 | 0.04 | 0.42 | 0.01 | 0.10 | 0.01 | Bal. |

Approximately 2 kg of the alloy was melted in a graphite crucible at 720 °C. A stirring impeller inserted at the bottom of the crucible was used at a low speed (<100 r/min) to homogenize the temperature of the melt in the crucible. Five thermocouples were used to record the temperatures at various positions as illustrated in Fig.3. The temperature data were recorded using Winview software through a data acquisition board. The gas induced semi-solid (GISS) process was used to create semi-solid slurry. In the GISS rheocasting process, a graphite diffuser was immersed into a molten metal held at a temperature above the liquidus temperature. In this work, the starting rheocasting temperature was 620 °C. Nine levels of solid fractions were obtained by varying rheocasting times ( $t_R$ ) of 1, 5, 10, 15, 20, 30, 35, 40 and 45 s. To capture the instant microstructure, the rapid quenching method was used. This method had been previously used in several studies[1]. The rapid quenching mold is shown schematically in Fig.3. The high cooling rates achieved by the mold allowed the capture of the microstructure at a temperature. The channel thickness of the quenching mold of 1 mm was used for the short rheocasting times of 1, 5, 10, 15, 20, and 30 s. Longer rheocasting times of 35, 40, and 45 s yielded the semi-solid slurry with the viscosity too high that the quenched samples mostly consisted of segregated liquid phase. Thus, the channel thickness of the quench mold was increased to 3 mm to obtain

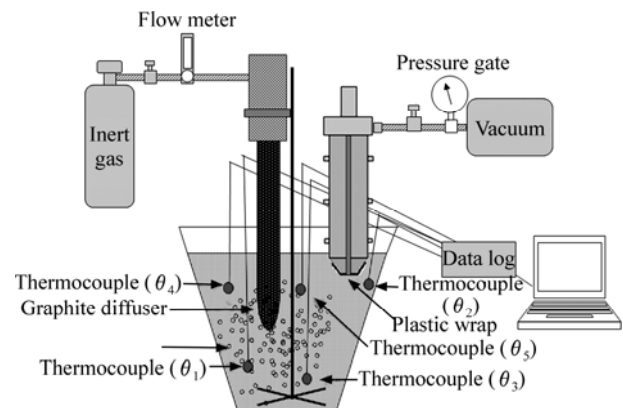


**Fig.3** Schematic diagram of experimental setup

homogeneous semi-solid samples. For each rheocasting time, 3 samples were obtained for further analysis.

Metallographic examination of the quenched samples was performed at the top, middle and bottom locations of the quenched plates, as illustrated in Fig.4. Standard grinding and polishing processes were conducted. The samples were then etched with 2% HF water solution for 9–12 s. The microstructure of the samples was captured using an optical microscope equipped with an image acquisition system. An image processing software was used to adjust the brightness and contrast of the captured micrographs. Quantitative image analysis was then performed on the micrographs using Image Tool software.

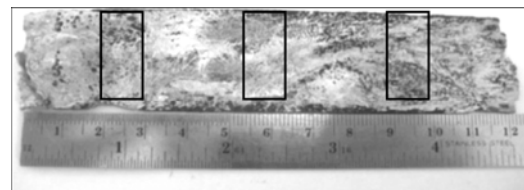


**Fig.4** Quenched plate and sample locations

### 4 Results and discussion

Representative sets of temperature distribution in the experiments are given in Table 2. For example, for the rheocasting time of 10 s, the temperatures at different locations in the melt are 614.3, 615.6, 615.9, 616.2 and 613.0 °C. The results show that the temperatures at different locations are not exactly the same. There are still pools of liquid metal with different temperatures even though agitation is applied to the melt.

Representative microstructures of the samples obtained at different rheocasting times are shown in Fig.5.

Observation on the microstructure shows that a mixture of globular, equiaxed, and dendritic particles are dispersed in the microstructure. The results in Table 2

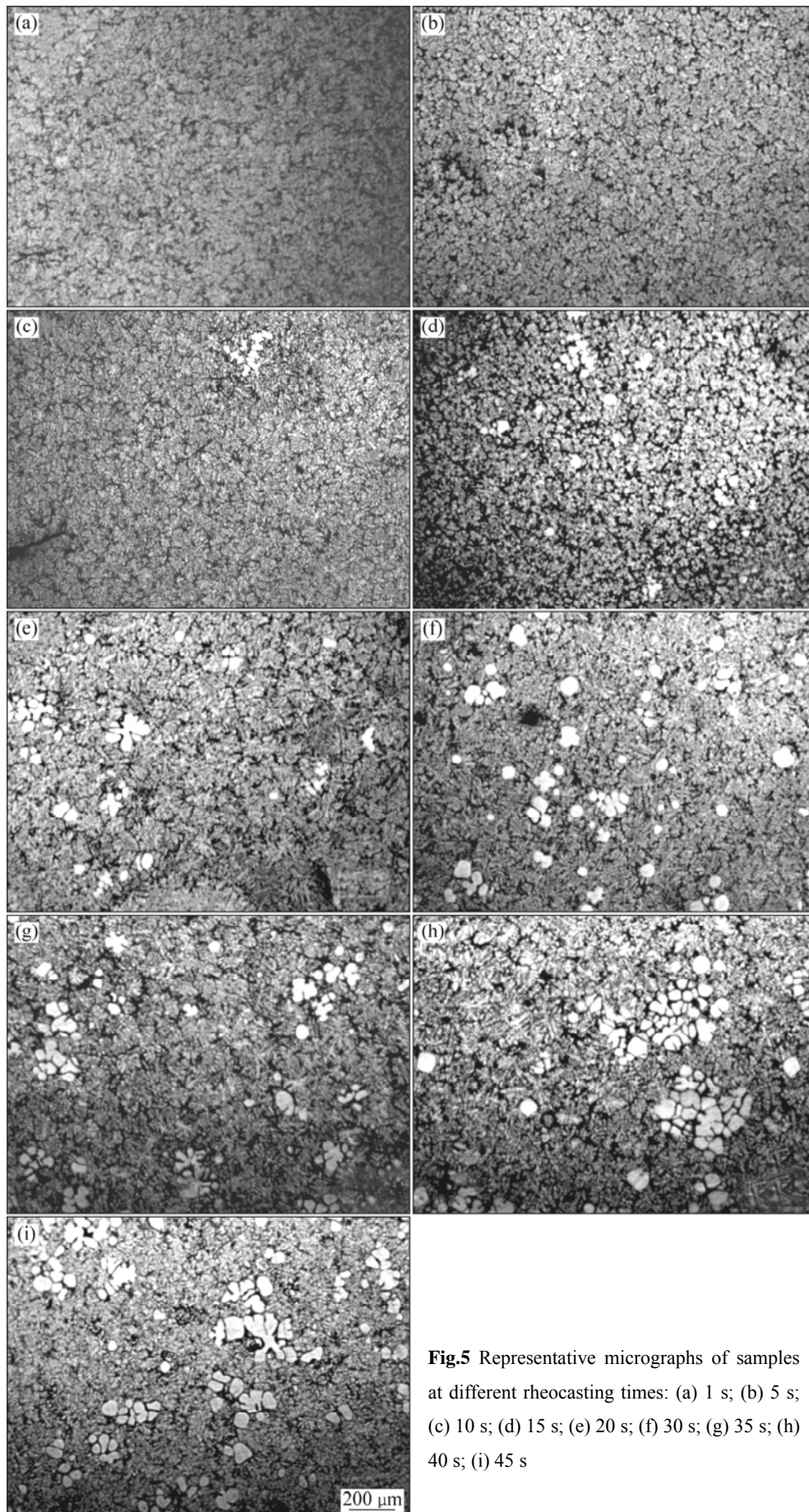


**Fig.5** Representative micrographs of samples at different rheocasting times: (a) 1 s; (b) 5 s; (c) 10 s; (d) 15 s; (e) 20 s; (f) 30 s; (g) 35 s; (h) 40 s; (i) 45 s

**Table 2** Solid fractions and representative temperature distribution in slurry at different rheocasting times

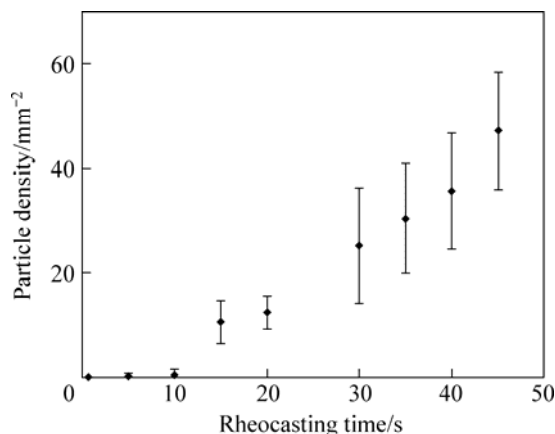
| Rheocasting time/s | Temperature distribution in slurry/°C |            |            |            |            | Average solid fraction/% |
|--------------------|---------------------------------------|------------|------------|------------|------------|--------------------------|
|                    | $\theta_1$                            | $\theta_2$ | $\theta_3$ | $\theta_4$ | $\theta_5$ |                          |
| 1                  | 619.2                                 | 620.6      | 618.7      | 620.7      | 620.2      | 0                        |
| 5                  | 619.3                                 | 620.3      | 620.8      | 618.4      | 617.8      | 0.01                     |
| 10                 | 614.3                                 | 615.6      | 615.9      | 616.2      | 613.0      | 0.05                     |
| 15                 | 611.5                                 | 612.5      | 611.8      | 611.4      | 611.9      | 2.05                     |
| 20                 | 610.1                                 | 612.3      | 610.1      | 611.7      | 611.6      | 2.78                     |
| 30                 | 612.5                                 | 613.4      | 612.1      | 612.5      | 611.9      | 5.55                     |
| 35                 | 611.5                                 | 607.4      | 608.7      | 609.8      | 609.0      | 7.89                     |
| 40                 | 609.1                                 | 604.0      | 606.5      | 603.1      | 602.8      | 10.86                    |
| 45                 | 608.9                                 | 602.2      | 606.3      | 603.5      | 602.7      | 14.58                    |

show the final solid fractions of 0, 0.01%, 0.05%, 2.05%, 2.78%, 5.55%, 7.89%, 10.86% and 14.58% for the rheocasting times of 1, 5, 10, 15, 20, 30, 35, 40 and 45 s, respectively. The solid fraction increases as the rheocasting time increases as expected, since cooling is continually achieved, resulting in reduced temperatures, thus, increased solid fractions.

#### 4.1 Effect of rheocasting time on particle density

The number of solid particles analyzed by quantitative image analysis as a function of the rheocasting time is summarized in Fig.6. The number of solid particles per square millimeter is 0, 0, 1, 11, 12, 25, 31, 36 and 47 for the rheocasting time of 1, 5, 10, 15, 20, 30, 35, 40 and 45 s, respectively. From these results, it can be noted that during the early rheocasting times of 1, 5 and 10 s, there are only a few solid particles in the melt. However, when the rheocasting time reaches 15 s, a significant increase in the solid particle density is obtained (from 1 to 11 mm<sup>-2</sup>). After that, the increase in the solid particle density is quite steady.

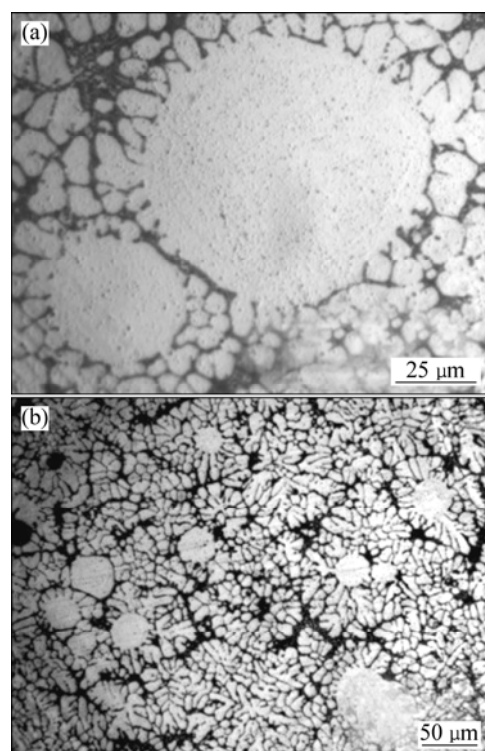
This interesting result may be explained by the fragmentation mechanism that once the cold graphite diffuser is inserted into the melt held at a temperature

**Fig.6** Effect of rheocasting time on particle density

slightly above the liquidus temperature, a large number of fine dendritic grains will be created near the cold surfaces and pushed away into the bulk liquid by the gas bubbles. During the early time of 1–10 s, the melt temperatures are still above the liquidus temperature. Thus, these mother dendrites will be remelted. However, remelting will take some time and there may be some pockets of undercooled liquid in the melt. So, there are some disintegrated or fragmented dendrite arms left in the melt as shown in the micrographs in Figs.5(a)–(c) even though the temperatures in the melt are above the liquidus temperature. When all the regions of the melt are not superheated (at the rheocasting times of 15 s and longer, see Table 2), a lot more fragmented arms from the remelting action can survive in the melt as observed in Fig.5(d). This action of remelting that yields the microstructure shown in Fig.5(d) can be explained schematically in Fig.2.

#### 4.2 Effect of rheocasting time on spherical particle density

Close examination of the microstructure indicates that there are a lot of fine spherical particles in the mixture of equiaxed and dendritic particles. Fig.7 gives representative microstructures showing the spherical particles. From the quantitative analysis, the average number of spherical particle per square millimeter is 0, 0, 0.20, 2.27, 2.66, 3.80, 3.81, 3.83 and 3.75 for the rheocasting time of 1, 5, 10, 15, 20, 30, 35, 40 and 45 s,

**Fig.7** Representative microstructures of spherical particles: (a) In high magnification; (b) In low magnification

respectively. These results are also plotted in Fig.8. It can be noticed that the spherical particle density also significantly increases from the rheocasting time of 10 to 15 s. The increase continues until the rheocasting time of 30 s. After this time, the number of spherical particles appears to be roughly constant. These experimental results may be explained by the fragmentation mechanism.

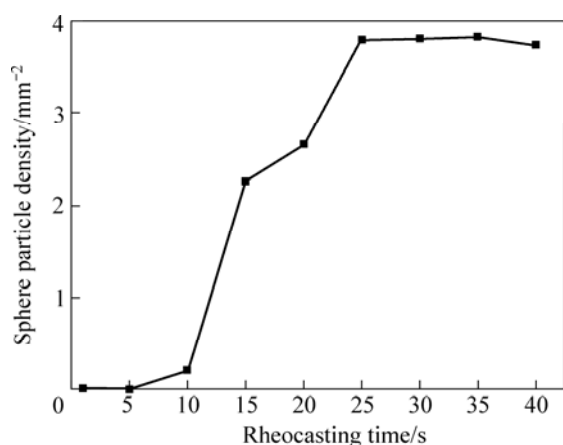


**Fig.8** Effect of rheocasting time on spherical particle density

The fragmentation by remelting mechanism suggests that some spheroidal particles will definitely be created at the early stages from the detached secondary or tertiary dendrite arms. The schematic of this mechanism shown in Fig.2 predicts that the microstructure after fragmentation by remelting should consist of a mixture of dendritic, equiaxed and globular particles. A coarsening model, shown in Fig.9, also suggests the formation of spheroidal particles after a remelting event.



**Fig.9** Dendrite coarsening model[16]

Sintering and coalescence of solid particles also occur in the slurry. During the fluid flow, solid particles may hit one another and sinter together. Fig.10 shows clumps of sintered particles. This phenomenon may explain why the spherical particle density remains constant as the rheocasting time increases. Although fragmentation may continue, yielding more spheroidal particles, the particles may be sintered together to form non-spherical clumps of particles. As the solid fraction increases, the chance for coalescence of particles is greater. Fig.11 shows examples of sintered particles that

are observed in the later rheocasting times in this work. Thus, from the results, it may be concluded that fragmentation of dendrite arms is continuously active in the early stages of the rheocasting process.



**Fig.10** Clumps of sintered particles[17]

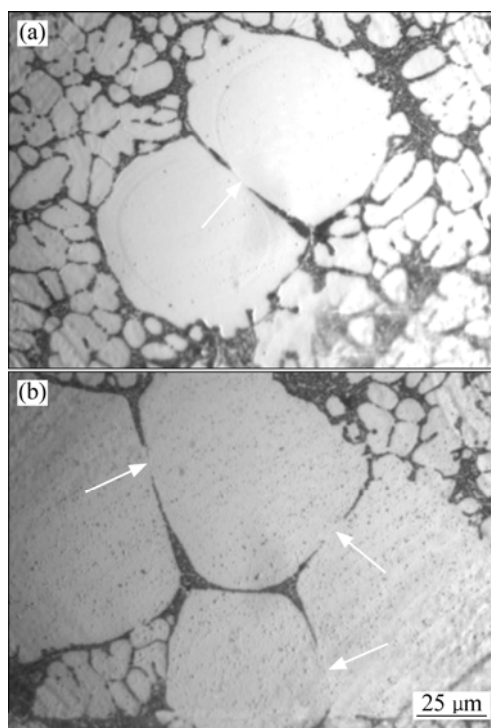


**Fig.11** Examples of sintered particles (Arrows indicate weld joints)

## 5 Conclusions

1) The microstructure at the early stages of a rheocasting process consists of a mixture of spheroidal, equiaxed and dendritic particles.

2) During the early rheocasting times, a few solid particles are observed in the melt even though the temperature in the melt is higher than the liquidus temperature. This may be because of incomplete remelting of the dendrites formed by the rheocasting process. After all the temperatures in the melt decrease below the liquidus temperature, significantly more solid grains can survive and are present.

3) The density of spherical particles increases as the rheocasting time increases and remains constant after a certain rheocasting time. The results suggest that the fragmentation by remelting mechanism is responsible for producing the observed spherical particles. The reason for the constant spherical particle density may be because of particle sintering when the solid fraction is increased.

4) The rapid quenching mold technique can be used to study the microstructure evolution of semi-solid slurries at the early stages. The information obtained may give more understanding in the formation mechanism of semi-solid metal microstructure.

## Acknowledgements

This work is funded by the Thai Research Fund (Contract No. MRG5280215) and the Royal Golden Jubilee Ph.D. Program (Grant No. PHD/0134/2551). The authors thank Mr. Songyot Jantawadee and the Innovative Metal Technology team for helping with the experiments and data analysis.

## References

- [1] JORSTAD J L. SSM processes — An over view[C]//The 8th International Conference on Semi-Solid Processing of Alloys and Composites. Limassol, Cyprus, 2004.
- [2] KIRKWOOD D H, SUERY M, KAPRANOS P, ATKINSON H V, YOUNG K P. Semi-solid processing of alloys [M]. New York: Springer Heidelberg Dordrecht, 2009.
- [3] WANNASIN J, CANYOOK R, BURAPA R, FLEMINGS M C. Evaluation of solid fraction in a rheocast aluminum die casting alloy by a rapid quenching method [J]. Scripta Materialia, 2008, 59: 1091–1094.
- [4] de FIGUEREDO A. Science and technology of semi-solid metal processing [M]. Rosemont: The North American Die Casting Association, 2001.
- [5] IQBAL N, VAN DIJK N H, OFFERMAN S E, MORET M P, KATGERMAN L, KEARLEY G J. Real-time observation of grain nucleation and growth during solidification of aluminum alloys [J]. Acta Materialia, 2005, 53: 2875–2880.
- [6] C.I.T, MOTEGI T, TANABE F. New semi-solid casting of copper alloys using an inclined cooling plate [C]//The 8th International Conference on Semi-Solid Processing of Alloys and Composites. Limassol, Cyprus, 2004.
- [7] LI T, LIN X, HUANG W. Morphological evolution during solidification under stirring [J]. Acta Materialia, 2006, 54: 4815–4824.
- [8] WU S, XIE L, ZHAO J, NAKAE H. Formation of non-dendritic microstructure of semi-solid aluminum alloy under vibration [J]. Scripta Materialia. 2008, 58: 556–559.
- [9] JIAN X, XU H, MEEK T T, HAN Q. Effect of power ultrasound on solidification of aluminum A356 alloy [J]. Materials Letters, 2005, 59: 190–193.
- [10] FLEMINGS M C, YURKO J, MARTINEZ R. Semi-solid forming: Our understanding today and its implications for improved process [C]//The 8th International Conference on Semi-Solid Processing of Alloys and Composites. Limassol, Cyprus, 2004.
- [11] HELLAWELL A, KIRKWOOD D H, KAPRANOS P. [C]// The Fourth International Conference on Semi-solid Processing of alloys and Composites. Sheffield: University of Sheffield, 1996: 40.
- [12] JACKSON K A, HUNT J D, UHLMANN D R, SEWARD T P. On the origin of the equiaxed zone in casting [J]. Transactions of the Metallurgical Society of AIME, 1966, 236: 149.
- [13] JI S. The fragmentation of primary dendrites during shearing in semisolid processing [J]. Materials Science, 2003, 38: 1559–1564.
- [14] RUVALCABA D, MATHIESEN R H, ESKIN D G, ARNBERG L, KATGERMAN L. In situ observations of dendritic fragmentation due to local solute-enrichment during directional solidification of an aluminum alloy [J]. Acta Mater, 2007, 55: 4287–4292.
- [15] MARTINEZ R A, FLEMINGS M C. Evolution of particle morphology in semi-solid processing [J]. Metallurgical and Materials Transactions A, 2005, 36: 2205–2210.
- [16] FLEMINGS M C. Solidification processing [M]. New York: McGraw-Hill Book Company, 1974.
- [17] NAFISI S, GHOMASHCHI R. The microstructural characterization of semi-solid slurries [J]. JOM, 2006, 58: 24–30.

(Edited by YANG Bing)